# THE NANOBALANCE TEST-STAND FOR MICRO-THRUST MEASUREMENTS: DIGITAL CONTROL AND DATA PROCESSING

*L. Massotti, E. Canuto*
Dipartimento di Automatica e Informatica, Politecnico di Torino
Corso Duca degli Abruzzi 24, 10129, Torino, Italy

This paper is concerned with a new instrument, the Nanobalance (NB), measuring thrust and noise time profiles of micro-thrusters (MT) for space applications in the range from 1 $\mu N$ to 1 $mN$ with submicronewton resolution, repeatability and accuracy better than $1\,\mu N/\sqrt{Hz}$ . The measurement accuracy shall be guaranteed in the frequency bandwidth from 0.1 $mHz$ to 2 $Hz$, called the instrument measurement bandwidth (MBW). MT with noise below the above accuracy, will be essential for upcoming "drag-free" missions like SMART-2 (Small Mission for Advanced Research in Technology, a technology demonstrator for LISA and Darwin [1]), LISA (Laser Interferometry Space Antenna, aiming to detect gravitational waves [2]) and Darwin (aiming to find Earth-like planets).

Previously, direct measurement of the thrust provided by MT with the above accuracy, either cold-gas or accelerated electric charge (as FEEP: Field Electric Emission Propulsion), was not possible through conventional thrust test-stands. In the last few years, several micronewton thrust stands have been developed in different facilities including, among the others, the Jet Propulsion Laboratory [3] and NASA Goddard Space Flight Center [4] in USA, and ONERA [5] in France. The most common thrust stands consist of a torsional pendulum operating in vacuum and carrying the MT and its balancing mass: a suitable position sensor, either optical or capacitive, measures the pendulum angular position.

The Nanobalance as shown in figure 1, was conceived and built by the *"*G. Colonnetti*"* Metrology Institute, Alenia Spazio and Politecnico di Torino (Italy), in order to exploit the high-sensitivity of in-vacuum Fabry-Pérot (FP) interferometers to sub-nanometric displacements [6]. Two parallel metallic plates suspended to an athermic spacer by flexible joints, carry the optical reflectors of a FP cavity wherein a laser beam is injected. Referring to figure 2, the active plate carries the micro-thruster under test, whereas the passive plate carries a dummy thruster in order to balance inertia and resonance of both plates. If perfectly balanced, both plates keep a steady distance as imposed by the athermic spacer, although oscillating under the effect of seismic

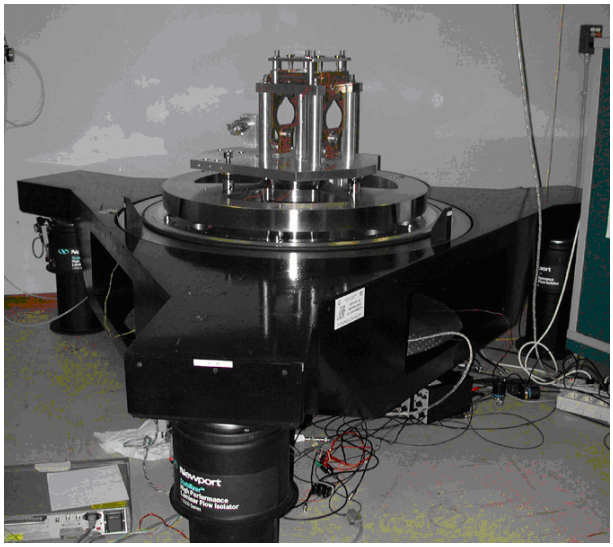

Fig. 1

noise. On the contrary, any nonzero thrust of the MT under test, displaces the active plate and reduces the cavity optical length: this effect is accurately sensed by the interferometric device.

It must be noticed that no contrasting actuator is needed (as in traditional thrust stands), thus avoiding the actuator noise. The MBW is limited by the plate resonance frequency, actually around 12 Hz, depending on the total plate and MT inertia plus the joint stiffness and harness. A critical point is the need of a careful plate balancing each time a new MT is mounted on the NB plates: other unbalanced forces are either negligible with respect to actual requirements (thermal noise) or dominated by constant terms (self-gravity, gravity gradient, electromagnetic coupling), falling into the offset calibration.

After an overview about the basic principles of the Fabry-Pérot interferometry, the paper firstly examines the thrust measuring principles and requirements, and then the instrument automation based on the Embedded Model Control (EMC) architecture, which provides the NB facility with different real-time functionalities, such as raw measures processing and calibration. Then, the attention is focused on the methods used for data reduction and on a significant example of test measurement and data processing.

## Fabry-Pérot Interferometry

Fabry-Pérot interferometer (FPI) was originally invented to enable high resolution observation of spectral lines. Several technological improvements were introduced during the XX century (for instance piezo-tuning the FPI optical length and introducing laser sources): in particular, FPI made by vacuum cavities between two highly reflecting mirrors have been suggested as metrology lines for stabilizing linear and angular dimensions of space telescopes like GAIA ([7], [8]).

FPI used for this particular task is an optical cavity [9] accomplished through two aligned and high reflecting mirrors merged in a vacuum chamber: a laser light-wave is injected inside them and a standing reflecting wave is maintained either regulating the frequency of the source beam or finely moving both mirrors. Consequently, the cavity becomes an optical resonator, because the injected light intensity is amplified inside the cavity mirrors having very low losses: the intensity amplification is measured by the *cavity finesse* $\mathcal{F}$ [9] which depends on the mirror reflectivity and can reach values greater than $10^4$.

The basic principle of the FPI is that any frequency perturbation of the incident light-wave as well as any perturbation of the optical path inside the cavity (due, for instance, to the micro-thruster when it is actuated) tends to destroy the resonant condition: as a consequence, the intensity of the light emitted by the cavity itself varies and a suitable opto-electronics allows to measure the perturbation amplitude and sign. Approaching mathematically the problem, let $f_1 = c/\lambda_1$ be the incident light frequency, typically from 200 to 600 *THz* (from infrared to green), related to the wavelength $\lambda_1$ by the speed of light $c$ in vacuum. Then denoting the cavity length with $L$ (typically from 0.01 to 100 *m*), measured along the optical axis joining the spot centres of the laser beam on each mirror, the standing wave condition implies an integer ratio between length and wavelength $L = N\lambda_1/2$, where $N$ in an integer. Equivalently,

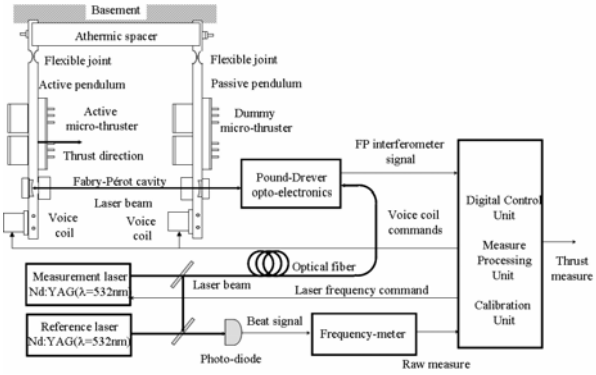


Fig. 2

multiplying $L$ times the incident light frequency, yields

$$f_1 L = Nc/2$$

A pair $(f_1, L)$ satisfying the above resonant condition is called a resonant pair and will be denoted as $(f_0(N), L_0(N))$. From the relationships written above, two successive resonant pairs $(N,\ N\pm1)$ are separated in length by half-wavelength $\lambda_0/2 = 266\ nm$ (Nd:YAG laser source) and in frequency by the so-called Free Spectral Range (FSR):

$$F_0 = 0.5\, c / L_0$$

where $F_0 \cong 750$ MHz @ $L_0 \cong 0.2$ m.

The standing wave condition can not be exactly met, but only approached by forcing frequency and length to fluctuate around a resonant pair through the active control. Thus by denoting length and frequency fluctuations (usually called detuning) with $\Delta L = L - L_0(N)$ and $\Delta f = f - f_0(N)$, and fractional detuning with $\eta$, the standing wave condition can be rewritten as

$$(f_0 + \Delta f)(L_0 + \Delta L) = f_0 L_0 (1+\eta)$$

as a linear differential equation relating length and frequency detuning. The cavity detuning $e$ can be introduced manipulating the previous expression:

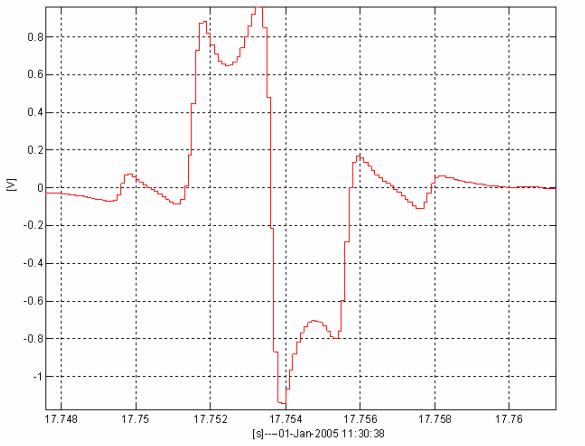


Fig. 3

$$\Delta f + (f_0 / L_0)\Delta L = e,\ \ e = f_0 \eta$$

This relation is called lock-in condition and holds under sufficiently small detuning $e$ (where small is dictated by cavity finesse $\mathcal{F}$). In this application, the cavity detuning $e$ plays the role of the performance variable (namely the control error) to be kept close to zero and below a predefined tolerance within a frequency bandwidth. As an example, the output signal of the interferometer is drawn in fig. 3: lock-in condition occurs when the signal is around the zero of the central slope.

## Thrust measuring principle

Nanobalance is made by two Copper-Beryllium alloy plates, which have to be as much as possible equal in geometry and density. Their upper pivots are flexible joints, kept at constant distance by an "athermic" spacer. The MT under test, providing a thrust $F_t(t)$, is mounted on the active pendulum (the left one in fig. 2); in order to balance the active MT, a dummy one is mounted on the passive pendulum (the right one). For calibration, the moving coil of a linear motor (voice coil) is mounted on each pendulum. Moreover, a pair of optical reflectors, one for each plate, sets up the FP cavity and works as the fine displacement sensor of the instrument [8].

When the active MT is switched on, the nonnegative commanded thrust $F_t(t) \geq 0$ causes a finite angular displacement between active and passive pendulum and a consequent detuning $\Delta L(t)$ of the optical path length $L(t)$ inside the FP cavity. If detuning occurs when the cavity length $L(t)$ is close to the resonance length $L_0$, $\Delta L(t)$ can be detected as a frequency variation $\Delta f(t)$ less the frequency error $e(t)$, as expressed in the previous section. This is accomplished by the Pound-Drever-Hall optoelectronics [10], which provides a voltage signal $y(t)$ -namely the FP interferometer signal- which is proportional to the cavity detuning $\Delta L(t)$. Then, $y(t)$ is employed as the error signal for driving a digital control unit (DCU) and a frequency actuator (a PZT ceramics), in order to change the laser source frequency $f(t) = f_0 + \Delta f(t)$ and keep the cavity close to a resonant condition.

In general, the thrust time-profile is accurately measured only in the MBW

$$F = \{f_l \leq f \leq f_h\}, f_l \geq \frac{1}{H}, f_h \leq F_1$$

bounded by the measurement horizon H ($\geq 10000\,s$) and the resonance frequency $F_1$ ($\cong 12\,Hz$) of the active pendulum. Due to the pendulum dynamics, the cavity detuning and the thrust are proportional (in the MBW) less the thermomechanical noise $d(t)$, due to seismic noise and thermoelastic deformations:

$$\Delta L(t) = -K_1 F_t(t) + d(t)$$

where the minus sign implies that the cavity length is reduced for a nonzero thrust $F_t(t) > 0$ and the proportionality constant $K_1$ depends on resonance and equivalent mass of the active pendulum. Inserting the expression of the control error in the previous expression, the fundamental thrust-to-frequency linear relation is obtained:

$$\Delta f(t) = K_b F_t(t) + d_f(t)$$

being $K_b$ the NB scale factor to be calibrated and $d_f(t)$ the sum of the thermomechanical noise *d* and the control error *e*. Finally, the laser frequency $f(t)$ encoding the frequency variation $\Delta f(t)$, is measured by "beating" the measurement laser together with a reference laser source, whose radiation frequency $f_r(t) = f_{0r} + \Delta f_r(t)$ is stabilized confining drastically the frequency fluctuations $\Delta f_r(t)$ in the MBW, below an adequate bound. The resulting radiation is then converted into an electric signal by a photodiode and the absolute frequency difference $|f_r(t) - f(t)|$ is averaged and sampled by a frequency-meter at discrete times $iT_f$. Thus, the output signal

$$y_f(i) = \Delta f(i) + v_f(i) + y_{f0}, y_{f0} = |f_{r0} - f_0|$$

is the raw instrument measure, being the sum of the useful signal $\Delta f(i)$, the offset $y_{f0}$ between reference and laser measurements, and the measurement noise $v_f(i)$, including frequency-meter errors and reference source fluctuations $\Delta f_r(t)$. Finally, the thrust measure of the $\Delta L(t)$ MBW components is provided by:

$$y_t(i) = \left(y_f(i) - \hat{y}_{f0}\right) / \hat{K}_b$$

upon the calibration of the scale factor $\hat{K}_b$ and of the offset $\hat{y}_{f0}$. Fig. 7 shows the instrument noise (called "reference") obtained during a MT test. The noise PSD (unilateral root Power Spectral Density) is well below $1\,\mu N/\sqrt{Hz}$ for frequencies from 1 *mH* to 1 *Hz*. The drift below 1 *mH* is under study to the end of its attenuation.

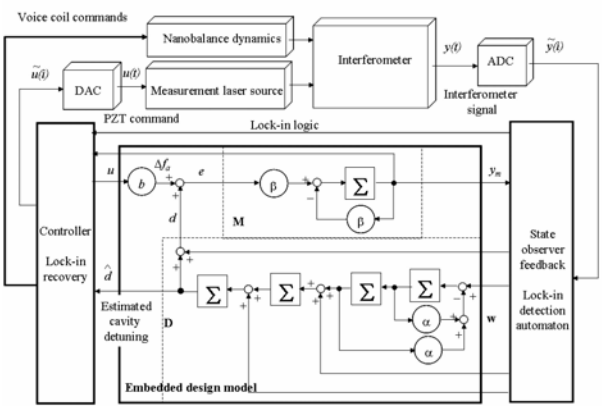


Fig. 4

## Instrument automation based on the Embedded Model Control (EMC)

The purpose of the automation design was to facilitate instrument setup for different measure scenarios every time that a new MT is mounted. In order to make measurements as accurate as possible, the scale factor and the offset must be calibrated: in particular, the last one may change from trial to trial, due to laser fluctuations. Another task is recognized as critical: the FP interferometer must be locked into the resonant length $L_0(N)$ at the onset and after shocks. Specifically, the lock-in function is implemented as a part of the digital control strategy [8]: traditionally, interferometer lock-in was manually set up and then preserved by analog loops designed *ad-hoc* to guarantee the required performance of the error $e(t)$. In this application, digital control was preferred to increase autonomy and performance.

Model/observer-based control algorithms are implemented at a 10 *kHz* rate, corresponding to a Nyquist frequency $f_{\max} = 5\,kHz$, and can be split into two groups: the linear controller and the lock-in detection and recovery. The former operates under quasi-linear conditions, which are established as soon as $e(t)$ comes within the interferometer linear range, namely the useful frequency region where the interferometer output signal becomes significantly nonzero and undergoes a sign change. The latter detects the prolonged presence of $e(t)$ outside the extended range and returns it to the linear range.

The core of the linear controller is the discrete-time (DT) embedded model (EM) shown in fig. 4 (synoptic scheme of the Digital Control Unit). The EM is the combination of the first-order controllable/observable dynamics **M**, mapping the control error $e(i)$ into the output $y_m(i)$ of the FP interferometer, and of the observable dynamics **D**: this one maps a white noise vector ***w***(i) into the DT signal $d(i)$, which represents the total frequency disturbance $\Delta f_d(t)$ (including also the laser source drift) to be tracked and rejected by the PZT voltage command *u*(i). **M** and **D** were realized as DT linear, time-invariant state equations in the form $x(i+1) = x(i) + u(i)$, represented through the symbol $\Sigma$ (DT integrator). In particular, **D** is a cascade of a pair of integrators and an oscillator, tuned at the resonance frequency $\sqrt{\alpha} = 2\pi F_1 T$ of the active pendulum. Whereas the integrators tend to model the MBW components of $\Delta f_d(t)$ due to laser drifts, thruster and thermomechanical noise, the oscillator models the pendulum beat due to background noise, which introduces mechanical noise components outside the MBW.

Control algorithms are driven by the model error

$$e_y(i) = y(i) - y_m(i)$$

expressed as the difference between the model output $y_m(i)$ and the real output $y(i)$, which is the sampled and digitalized $\tilde{y}(i)$ of the sensor voltage $y(t)$ converted into frequency units. The observer feedback (see fig. 4), driven by $e_y(i)$, provides a realization of the driving noise ***w(i)***, which, applied to the **DM**, estimates the disturbance signal $\hat{d}(i)$. In this way, the

controller computes the command $u(t)$ and its digital counterpart $\tilde{u}(i)$ as a linear combination of $\hat{d}(i)$ and $y_m(i)$:

$$u(i) = -\left[\hat{d}(i) + Ky_m(i)\right]/b$$

The first component of the control law cancels the nonstationary components of $d(i)$ from the DT control error $e(i)$, whereas the second one guarantees that the estimated residual $\hat{e}(i) = d(i) - \hat{d}(i)$ converges to a statistically bounded random process. Control parameters, i.e., the scalar gain $K$ and the observer feedback gains, were designed to be robust to the unmodelled dynamics, mainly due to the PZT actuation frequency [8]. The design methodology, following [11], exploits the filtering action of the state observer with regard to the de-stabilizing effect of the model error $e_y(i)$. The price to be paid is a limited region within the unit circle and close to 1 $(\approx 0.8 \div 0.95)$, where the observer eigenvalues can be placed, meaning a limited bandwidth where disturbances can be estimated and compensated. As these limits cannot be removed, disturbance estimation can only be improved by **D** designing to accurately fit the disturbance PSD within the available control bandwidth.

## Data reduction

Due to a digital control bandwidth (>100 Hz) much larger than the MBW, the raw measures provided by the frequency meter are corrupted by the higher-frequency components (> 10 Hz) of the mechanical noise $d(t)$, which is dominated by the beat motion, centered around $F_1$. An observer-based digital filter removes such components either in real time or off line, thus providing a faithful and recognizable time profile of the measured thrust within the MBW. The algorithm was

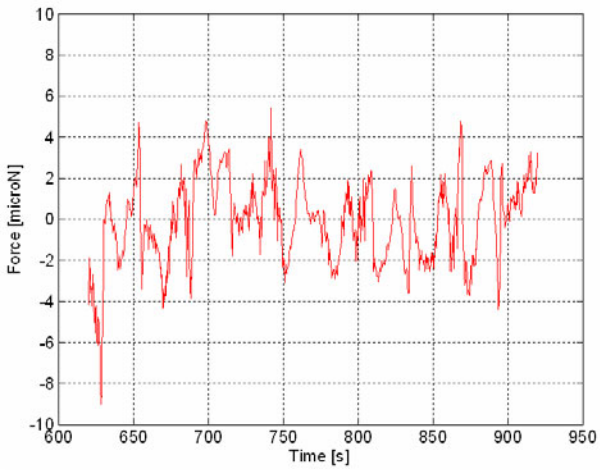


Fig. 6

built around the same disturbance dynamics **D** of the EM, but arranged in order to separate the MBW components $\Delta F(i)$ of the total thrust $\Delta F(t)$ from the pendulum beat motion centered on the DT adimensional frequency $2\pi F_1 T_f$, being $T_f$ the time unit of the frequency meter.

The thrust measure $\Delta F(i)$ is the output of the thrust/noise dynamics **D** accomplished through a cascade of two DT integrators, driven by the noise vector $\boldsymbol{w}(i)$ provided by the observer feedback. In particular, the latter is driven by the model error $e_t(i) = y_t(i) - \hat{y}_t(i)$ between the raw measure $y_t(i)$, converted into force units, and the estimated model $\hat{y}_t(i)$. It must be noticed that if the commanded thrust $F_t$ and voice coils dynamics were known, they could be removed from the thrust measure, by explicitly adding their contribution to the NB dynamics. Therefore the sampled MT noise $w_t(i)$ can be measured in the MBW from the following equation:

$$\Delta F(i) = w_t(i) - e_t(i)$$

where the instrument error is $e_t(i) = F_t(i) - y_t(i)$. The range of the filter eigenvalues, only limited by measurement noise, is $\approx 0.8 \div 0.9$.

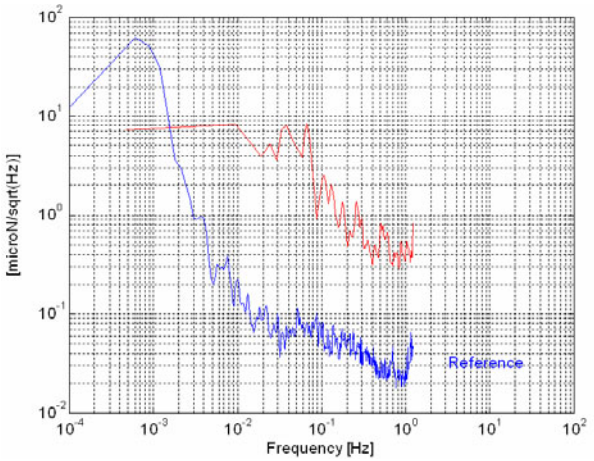


Fig. 7

## Experimental results

Experimental results refer to preliminary tests performed on the NB in view of several upcoming test campaigns. The first trials were focused on the instrument measurements without thrusters, successively a cold gas MT (balanced by a dummy one) was installed and data were collected using different thrust command profiles. A very preliminary test concerning the estimation of the maximum and minimum thrust, is shown in Fig. 5: the measured thrust was obtained by processing the raw measurements in order to de-trend raw data from instrument background noise. The residuals, visible in fig. 6, are obtained as the difference between raw data and measured thrust: the signal is affected by "almost" periodic oscillations due to phenomena under investigation, nevertheless the residuals RMS is close to 2 $\mu N$. Fig. 7 compares the PSD of the MT residuals (see upper bounds in table 1) to the instrument noise.

Table 1

| *Residuals* | Value (RMS) $[\mu N]$ | PSD upper bound $\lfloor \mu N / \sqrt{Hz} \rfloor$ |
|---|---|---|
| *e* | 2.1 | 8 |

It can be concluded that thrusts of the order of 1 $\mu N$ shall be measured for $f > 2\,mHz$, and finely appreciated until to 0.1 $\mu N$ for $f > 0.1\,Hz$. It has to be noticed that PSD are bounded to 1 *Hz* in order to cut the frequencies related to the pendulum beat.

## References

[1] Vitale, S., *et al. LISA and its in-flight test precursor SMART-2*. Nucl. Phys. B, Proc. Suppl. 110, pp. 209-216, 2002.

[2] LISA study team. *Laser Interferometer Space Antenna. A cornerstone mission for the observation of gravitational waves*. ESA SCI, 11, July 2000.

[3] Ziemer, J.K. Performance measurements using a sub-micronewton resolution thrust stand. *Proc. of the 27th International Electric Propulsion Conference*, Pasadena, CA, October 15-19 2001.

[4] Merkovitz, S.M., Maghami, P.G., Sharma, A., Willis, W.D., and Zakrzwski, C.M. *A μNewton thrust-stand for LISA*. Class. Quantum Grav. 19, pp. 1745-1750, 2002.

[5] Bonnet, J., Marque, J.P., and Ory. M. Development of a thrust balance in the micronewton range. *Proc. Of the 3rd International Conference on Spacecraft Propulsion*, Cannes, France, edited by R.A. Harris, ESA SP-465, October 10-13 2000.

[6] Bertinetto, F., Canuto, E. *Sub-nanometer digital positioning of large bodies by Fabry-Pérot interferometry*. Opt. Eng. (Bellingham), 40 (1), pp. 76-80, 2001.

[7] Canuto, *E. Sub-nanometric optics stabilization in view of the GAIA astronometric mission*. Control Eng. Practice, 11(5), pp 569-578, 2003.

[8] Canuto, E., Rolino, E. Nanobalance: An automated interferometric balance for micro-thruster measurement. *ISA Trans*., 43 (2), pp. 169-187, 2004.

[9] Siegman, A.E. *Lasers*. Sausalito (CA): Univ. Science Books, 1986.

[10] Drever, R.W., Hall, J.L., Kowalski, F.W., Hough, J., Ford, G.M., Munley, A.J. *et al. Laser phase and frequency stabilization using an optical resonator*. Appl. Phys. B: Photophys. Laser Chem., 21, pp. 97-105, 1983.

[11] Donati, F., Vallauri, M. Guaranteed control of 'almost-linear' plants. *IEEE Trans. Autom. Control*, 29, pp. 34-41, 1984.